

Effect of index of refraction mismatch on the recovery of optical properties of cylindrical inhomogeneities in an infinite turbid medium.

Scott A. Walker*, Sergio Fantini, and Enrico Gratton

Laboratory for Fluorescence Dynamics
Department of Physics, University of Illinois at Urbana-Champaign
1110 W. Green St., Urbana IL 61801-3080

ABSTRACT

Optical inhomogeneities embedded in a turbid medium are characterized not only by their absorption and reduced scattering coefficients, but also by their index of refraction relative to the background medium. Although in diffusion theory it is impossible to separate the index of refraction from the absorption and reduced scattering coefficients in an infinite homogeneous medium, application of boundary conditions for an inhomogeneity adds enough information to separately determine these optical properties. A mismatched index of refraction affects diffuse photon propagation in two ways: photons travel at a different speed inside the inhomogeneity, and photons entering and leaving the inhomogeneity are influenced by Fresnel reflections at the surface of the object. We have integrated these two effects into the analytical solution to the diffusion equation for a cylinder in an infinite medium. Theoretical results are compared with experimental data, and the effect of index of refraction mismatch is evaluated for different combinations of optical properties.

Keywords: photon migration, near-infrared optical tomography, frequency domain imaging, index of refraction, Fresnel reflection, boundary conditions.

1. INTRODUCTION

Index of refraction (n) of tissues is experimentally important in the determination of optical properties such as specular reflectivity, angular change in beam direction at tissue interfaces, and acceptance angles of optical fibers in tissue. The index of refraction has been determined for many different human tissues with a majority of values ranging from $n=1.35$ to $n=1.45$ at a wavelength of 632.8 nm.^{1,2,3,4} Values for tissue indices of refraction have both been measured in vitro using a quartz optical fiber¹, and estimated based on the water content of tissue.⁴ These different values of n not only affect light propagation at the surface of diffuse media but also at any inhomogeneity inside the medium.

While the effect of an index of refraction mismatch at the surface of a turbid medium has been studied, little experimental work has been done to verify the effect of an index mismatch at a boundary of an inhomogeneity inside a turbid medium. Haskell *et al.*⁵ predicted that the index of refraction will modify boundary conditions inside a turbid medium such that only the normal component of the flux will be continuous across boundaries, but not the fluence rate. Some of the light incident on the boundary will undergo Fresnel reflection depending on the index of refraction mismatch between the object and background media. We have included this modified boundary condition in the analytical solution for a cylinder in an infinite turbid medium and compare our theoretical solution with experimental data.

2. THEORY

We can describe the propagation of photons in a scattering medium with the Boltzmann transport equation. This equation can be simplified by a diffusion approximation to yield, in the frequency domain, for homogeneous media:⁶

$$\left(\nabla^2 + k^2\right)\Phi(\mathbf{r}, \omega) = -\frac{q(\mathbf{r}, \omega)}{D} \quad (1)$$

where,

* Further author information

S.A.W. (correspondence): Email: sawalker@uiuc.edu; WWW: <http://www.physics.uiuc.edu/groups/fluorescence/>
phone: (217)244-5620; Fax (217)244-7187

$$k^2 = \frac{-\nu\mu_a + i\omega}{\nu D} \quad (2)$$

Here $\Phi(\mathbf{r}, \omega)$ is the photon fluence rate, ω is the angular frequency of source modulation, $q(\mathbf{r}, \omega)$ is the source power per unit volume, and $\nu = c/n$ is the speed of light in the scattering medium (n is the index of refraction of the medium), μ_a is the absorption coefficient and $D=1/(3\mu_s)'$ ⁷ is the diffusion coefficient (μ_s' is the reduced scattering coefficient of the medium). The general form of the solution for a point source at position \mathbf{r}_s is:

$$\Phi(\mathbf{r}, \mathbf{r}_s, \omega) = S \frac{\exp(ik_{out}|\mathbf{r} - \mathbf{r}_s|)}{4\pi D|\mathbf{r} - \mathbf{r}_s|} \quad (3)$$

where S is the power of the source in photons/s. If we wish to solve the Helmholtz equation (Eq. 1) in the presence of an infinite cylinder we can expand the general solution (Eq. 3) in terms of modified Bessel functions.⁸ The fluence rate inside the cylinder (Φ_{in}), and the fluence rate resulting from the scattering of the incoming wave by the cylinder (Φ_{scatt}) will also be expanded similarly. This procedure follows the approach presented by other researchers for spherical inhomogeneities.^{9,10} We can determine the coefficients in the expansion by imposing the following boundary conditions ($\rho=a$ represents the cylinder surface):⁵

$$1. \quad \Phi_{scatt} \rightarrow 0 \text{ as } \rho \rightarrow 0 \quad (4)$$

$$2. \quad \Phi_{in} \text{ is finite everywhere} \quad (5)$$

$$3. \quad (1 - R_{21})\Phi_{out} = \left[(1 - R_{21}) + 2(R_{12} - R_{21})D_{in} \frac{\partial}{\partial \rho} \right] \Phi_{in} \text{ at } \rho = a \quad (6)$$

$$4. \quad D_{out} \frac{\partial}{\partial \rho} \Phi_{out} = D_{in} \frac{\partial}{\partial \rho} \Phi_{in} \text{ at } \rho = a \quad (7)$$

Where the subscripts "out" and "in" indicate whether the corresponding quantity is evaluated outside or inside the cylinder respectively. Here, ρ is the radial distance from the center of the cylinder, and a is the radius of the cylinder. R_{12} and R_{21} are effective reflection coefficients describing the fraction of emitted light that is reflected either out of or into the cylinder at a boundary due to Fresnel reflections (For the index of refraction mismatch in our experiment $n_{cylinder}=1.8$ vs. $n_{background}=1.33$, $R_{12}=0.45$ and $R_{21}=0.057$). Boundary condition 3 shows a discontinuity in the fluence rate at the object surface which depends on the effective reflection coefficients R_{12} and R_{21} .⁵ The discontinuity in Φ is due to the fact that not all of the light incident on the cylindrical boundary is transmitted into (or out of) the cylinder.

After matching the expanded solutions using the boundary conditions above one can arrive at an analytical solution for the case of an infinite cylinder in a turbid medium. This solution accounts for the effects of the index of refraction mismatch between the cylinder and the background medium in two ways: first the speed of light is changed in the inhomogeneity, and second Fresnel reflections cause a discontinuity in the fluence rate across the boundary between the cylinder and the background medium.

3. MATERIALS AND METHODS

Experimental measurements were conducted in a quasi-infinite geometry using a frequency domain spectrometer and an XYZ positioning scanner. A 120 MHz radio frequency signal was amplified and sent to a 50 mW laser diode ($\lambda=793$ nm) coupled to a 1 mm fiber optic conduit to channel the near infrared light into the turbid medium. The coupling efficiency with the laser diode was 20% giving an output power of about 10 mW. Detected light was collected by a 0.3 cm diameter fiber optic bundle and processed with frequency domain methods to measure the DC intensity, AC amplitude, and phase of the photon density wave. Measurements took place inside a large glass container of Intralipid fat emulsion mixed with black India ink. The volume of the container was 16 L. The concentrations of Intralipid and India ink were adjusted to give background optical coefficients $\mu_{a0}=0.079$ cm⁻¹, $\mu_{s0}=8.0$ cm⁻¹ as measured by the multidistance protocol.¹¹ The index of refraction of the medium is 1.33 (water).

To mimic infinitely long cylinders, we cast 5 cylinders each 10 cm long with 3 different radii (0.25 cm, 0.5 cm, and 0.75 cm) and having two sets of optical coefficients (Material A+: $\mu_{a1}=0.06$ cm⁻¹, $\mu_{s1}=5$ cm⁻¹; Material A-: $\mu_{a2}=0.18$ cm⁻¹, $\mu_{s2}=6$ cm⁻¹) (see table 1).

Medium	μ_a (cm^{-1})	μ_s (cm^{-1})	n
material A+	0.18 ± 0.02	6 ± 1	1.8 ± 0.1
material A-	0.06 ± 0.01	5 ± 1	1.8 ± 0.1
background medium (Intralipid + India ink)	0.079 ± 0.005	8.0 ± 0.1	1.33*

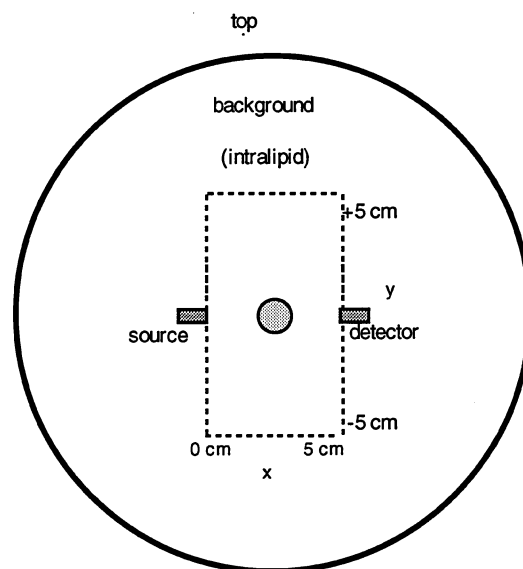
Table 1. Measured values of absorption and reduced scattering coefficients and index of refraction for experiment materials. Cylindrical inhomogeneities were made from hot melt glue, and the background medium was Intralipid fat emulsion mixed with India ink. *The value for index of refraction of the background medium is the value for water.

Each cylinder was made from a large block of Hot Melt glue which was characterized using a semi-infinite medium multidistance protocol.¹² Due to the optical coefficients of the background medium, the probability of a photon traveling from source to detector about the end of a cylinder is negligible. Thus we treat each cylinder as being infinitely long.

We performed an experiment to measure the index of refraction of the glue. After forming the clear glue into a right angle prism we directed light from a He-Ne laser ($\lambda=632.8$ nm) into the prism and measured the critical angle for total internal reflection. From this measurement we employed Snell's law to extract the index of refraction of the glue.

A set of experiments was performed to compare the theoretical model with experimental data. A single cylinder was located midway between source and detector, (as shown in Fig. 2).

Figure 1. Experimental Setup. Top view of the 16L glass container filled with Intralipid/India Ink mixture. Fiber optics carry light to and from the source and detector. The fiber tips are separated by 5 cm inside the tank and positioned by means of a mechanical XYZ scanner with a positioning accuracy of $10 \mu\text{m}$. The 1 cm diameter object is suspended by a 3 mm diameter glass rod at position $x=0.2$ cm and $y=0$ cm.



The phase and amplitude of the resulting photon density waves are recorded as the source and detector perform a linear scan across the object. Source and detector optical fibers are scanned in tandem, always facing each other, with a separation of 5 cm. Each scan consists of 51 measurements of the photon density wave taken at 0.2 cm steps for a total of 10 cm. Each scan was reproducible with a position error of $10 \mu\text{m}$ due the XYZ positioning scanner. The resulting data is fit by implementing the analytical solution shown above with a least squares fitting procedure inside the PMI public domain program developed at the University of Pennsylvania.⁹

After verifying that the analytical solution reproduces the experimental results, we plot solutions to this equation for a different experimental condition. We examine the effect of a large index of refraction mismatch ($n_{\text{object}}=1.8$, $n_{\text{background}}=1.333$) for a 1 cm diameter cylinder with absorption and reduced scattering coefficients equal to those of the background highly scattering medium.

4. RESULTS

4.1 Fit of μ_a , μ_s' and n for a given cylinder radius

Table 2 shows the values of absorption and reduced scattering coefficient that we recover assuming no index of refraction mismatch between the cylinders and the background medium.

radius (cm)	μ_a (cm ⁻¹)	μ_s' (cm ⁻¹)	n	(reduced χ^2) ¹³
type A+				
0.75	0.161	9.1	1.33	11
0.5	0.162	9.0	1.33	4.2
0.25	0.155	9.4	1.33	0.97
type A-				
0.75	0.046	6.9	1.33	31.4
0.5	0.054	6.9	1.33	9.1

Table 2. Best fit values of the absorption and scattering coefficients of the cylindrical inhomogeneities assuming the cylinder's index of refraction is the same as the background (see table 1 for the actual values). These values are obtained from a least squares fit of the analytical solution to the diffusion approximation to the Boltzmann transport equation ignoring the fact that the cylinders have an index of refraction different from the background medium. Experimental errors are 0.2% in the AC counts, and 0.1 degrees in the phase.

The radius of each cylinder is fixed to the correct radius while the absorption and reduced scattering coefficients of the cylinder material are varied to fit the theoretical model to the experimental data. The best fit values for absorption and scattering coefficients are different from the actual values because of the assumption of an incorrect index of refraction for the cylinder ($n=1.33$).

Using boundary conditions that do not take into account Fresnel reflections, it is virtually impossible to separate the effect due a change in the index of refraction from changes in the absorption and scattering parameters.⁴ In this case the independently measured quantities are essentially $n\mu_s$ and μ_a/n since these variables appear together in the diffusion approximation to the Boltzmann transport equation. Hence, the same reduced χ^2 values will be obtained for different combinations of values of μ_a , μ_s' , and n .

Table 2 is compared with table 3 which shows the agreement between theory and experiment for an infinite scattering cylinder in an infinite scattering medium when we take into account Fresnel reflections at the cylinder surface.

radius (cm)	μ_a (cm ⁻¹)	μ_s' (cm ⁻¹)	n	reduced χ^2
Material type A+				
0.75	0.183±0.005	7.1±0.1	1.7±0.05	2.0
0.5	0.181±0.007	6.4±0.2	1.75±0.08	0.95
0.25	0.17±0.03	6.6±1.2	1.65±0.4	0.94
Material type A-				
0.75	0.073±0.001	4.5±0.2	1.8±0.05	1.1
0.5	0.081±0.001	4.2±0.4	1.8±0.07	0.9

Table 3. Best fit values of absorption and reduced scattering coefficients and index of refraction of cylindrical inhomogeneities (see table 1 for the actual values). These values are obtained from a least squares fit of the analytical solution to the diffusion approximation including the effects of a mismatch in the index of refraction between the cylinders and the background medium. Experimental errors are 0.2% in the AC counts, and 0.1 degrees in the phase.

In general, independently measured values of the absorption and reduced scattering coefficients as well as the index of refraction of each cylinder are recovered within experimental error. The reduced χ^2 value for each fit serves as a measure of goodness of fit (experimental errors are 0.2% error in the AC counts and 0.1 degrees in the phase). Each cylinder is assumed to be at a known position with a vertical orientation. Note that the improvement in the reduced χ^2 , with the introduction of Fresnel reflections, is largest for the less absorbing cylinders of material type A-. The actual plot of experimental and theoretical values is shown for the 1.5 cm diameter cylinder of material type A- in Fig. 2 (a) and (b).

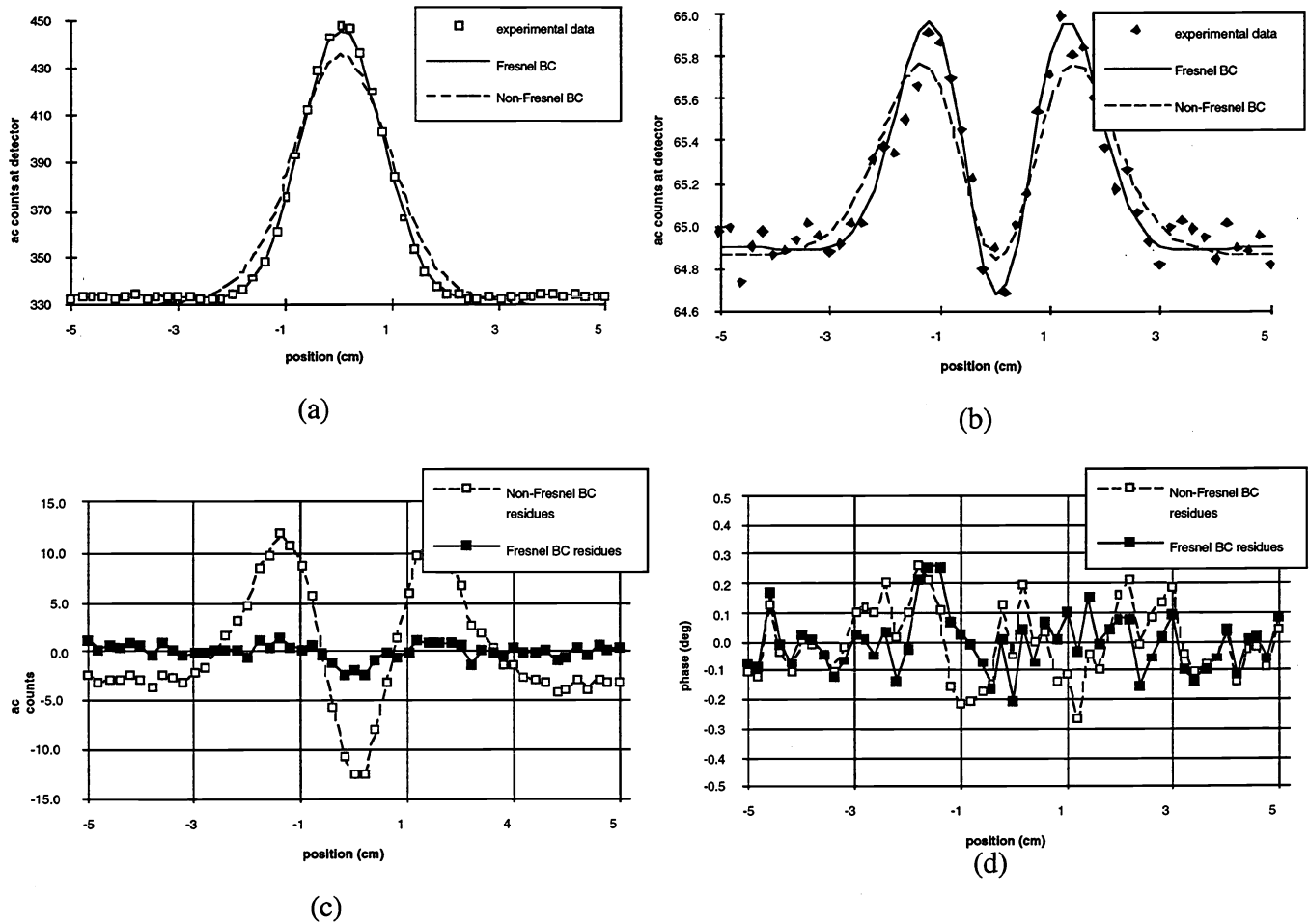


Fig. 2 Sample fits to the experimental data are presented for a 1.5 cm diameter cylinder with optical coefficients $\mu_a=0.06 \text{ cm}^{-1}$, and $\mu_s=5.0 \text{ cm}^{-1}$ and $n=1.8$. (a) The open squares represent the experimental measurements, while the dashed line represents the best fit of the theory to the experiment without taking into account Fresnel reflections at the cylinder's surface. The solid line is the best fit including Fresnel reflections. (b) The filled diamonds represent the measured phase while the solid (dashed) line shows the best fit of theory with (without) Fresnel reflections at the cylinder surface. (c) The filled squares represent the AC residues (model - experiment) for each measurement position using the Fresnel reflection model. The open squares reflect the larger residues for the model without Fresnel reflections. (d) Here the filled squares show the residues for the Fresnel model, while the open squares show the residues without Fresnel reflections.

Figures 2 (a) and (b) show a comparison between the fit obtained with the Fresnel reflection model with the non-Fresnel reflection model. Both fits assume an index of refraction $n=1.8$, however this choice of index of refraction is somewhat arbitrary for the model that does not include Fresnel reflections, since any change in refractive index of the cylinder can be compensated by changes in the absorption and scattering coefficients. The model including Fresnel reflections shows a slight narrowing in the cylinder's profile allowing for a better fit to the experimental data. The differences between model and experimental measurements (residues) are shown in Fig. 2 (c) and (d). The open squares in Fig. 2 (c) show a significant correlation among the residues for the model without Fresnel reflections. This correlation is greatly reduced by introducing the new boundary conditions which include Fresnel reflections, as shown by the filled squares. The residues in Fig. 2 (d) show that the fit is dominated by random error and the new boundary conditions decrease the χ^2 value only slightly.

This excellent agreement between theory and experiment, with the new boundary conditions, indicates that the diffusion approximation to the Boltzmann transport equation is sufficient to describe the transport of photons in a highly scattering medium even in the presence of inhomogeneities with sharp variations in absorption and reduced scattering coefficients as well as sharp variations in index of refraction.

4.2 Modeling the effect of an index of refraction mismatch for various experimental conditions.

Fig. 3 shows the effect of a large index mismatch ($n_{\text{object}}=1.8$, $n_{\text{background}}=1.333$) when object absorption and reduced scattering parameters are held equal to background values ($\mu_{a0}=0.1 \text{ cm}^{-1}$, and $\mu_{s0}=10 \text{ cm}^{-1}$). The dashed lines show measurements made in a tandem scan from -4 cm to 4 cm (see Fig. 2) of a 1.0 cm diameter cylinder centered between source and detector. Here we take into account only the fact that light travels slower inside the cylinder than in the background medium.

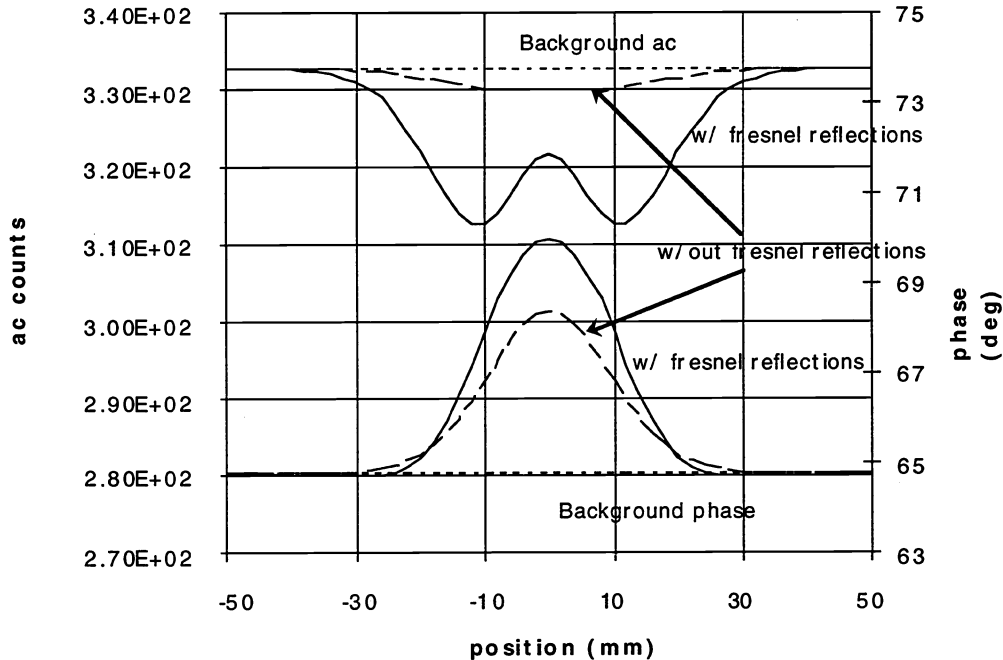


Fig. 3. Effect of an index of refraction mismatch for a 1.0 cm diameter cylinder with μ_a and μ_s the same as background values. The dotted lines show the values of the measured AC and phase for a background medium with optical properties $n=1.333$, $\mu_{a0}=0.1 \text{ cm}^{-1}$, and $\mu_{s0}=10 \text{ cm}^{-1}$ given a 5 cm source detector separation. The dashed lines show the effect of a 1.0 cm diameter cylinder ($n=1.8$, μ_a and μ_s same as background values) centered between source and detector, as they are scanned in tandem across the object from -4 cm to 4 cm (see Fig. 2). Here we take into account only the fact that light travels slower inside the cylinder than in the background medium. The solid lines show the AC and phase measurements taking into account both the slower speed of light in the cylinder and the effect of Fresnel reflections at the surface of the cylinder. The deviations from background values in both AC and phase are significant in terms of measurement error.

The solid lines in Fig. 3 show the AC and phase measurements taking into account both the slower speed of light in the cylinder and the effect of Fresnel reflections at the surface of the cylinder. The deviations from background values in both AC and phase are significant in terms of measurement error. Note that the addition of Fresnel reflections to the model results in a maximum 6% change in the detected AC counts as well and an double minimum in the AC profile of the cylinder. This unusual shape is probably due to the fact that Fresnel reflections are a surface effect and do not affect photons traveling through the center of the cylinder as strongly as those traveling near the cylinder/background interface.

5. CONCLUSION

Previously, highly scattering inhomogeneities have been characterized by two parameters, their absorption and reduced scattering coefficients. The index of refraction of an inhomogeneity could not be independently determined from optical measurements in a highly scattering medium. Any error in the assumed index of refraction affected the recovered values of absorption and reduced scattering coefficients because detected photons traveled at a different than expected speed inside the inhomogeneity. However, there is an added effect due to an index of refraction mismatch: photons entering and leaving the inhomogeneity are also influenced by Fresnel reflections at the surface of the object. This surface effect effectively sets photon migration theory apart from the diffusion theory of other non-interacting particles, such as neutrons, and allows us a possibility for independently determining the index of refraction of an inhomogeneity.

In this paper, we have corrected the boundary conditions for the diffusion approximation to the Boltzmann transport equation to include Fresnel surface reflections in the case of a mismatch in the refractive index between an infinite cylinder and its surrounding medium. These new boundary conditions lead to better fit of experimental data than with the old boundary conditions without introducing any significant complication. The model including Fresnel reflections allows us to separate the effects of a material's index of refraction from its absorption and scattering coefficients, effectively creating another parameter which should be separately determined to fully characterize the optical properties of a highly scattering inhomogeneity.

ACKNOWLEDGMENTS

This work was performed at the Laboratory for Fluorescence Dynamics at the University of Illinois at Urbana-Champaign (UIUC), which is supported by the National Institutes of Health (NIH), grant RR03155 and by UIUC. This research is also supported by grant CA57032 from the NIH.

REFERENCES

1. F. P. Bolin, L. E. Preuss, R. C. Taylor, and R. J. Ference, "Refractive Index of Some Mammalian Tissues Using a Fiber Optic Cladding Method," *Appl. Opt.* **12**, 2297-2302 (1989).
2. B. Beauvoit, T. Kitai, and B. Chance, "Contribution of the mitochondrial compartment to the optical properties of the rat liver: A theoretical and practical approach." *Biophysical Journal* **67**, 2501-2510 (1994).
3. H. Li, and S. Xie, "Measurement method of the refractive index of biotissue by total internal reflection," *Appl. Opt.* **35**, 1793-1795 (1996).
4. S. L. Jacques, C. A. Alter, and S. A. Prahl, "Angular Dependence of HeNe Laser Light Scattering by Human Dermis," *Lasers in Life Sci.* **1**, 309-333 (1987).
5. R. C. Haskell, L. O. Svaasand, T. Tsay, B. J. Tromberg, "Boundary Conditions for the Diffusion Equation in Radiative Transfer," *J. Opt. Soc. Am. A* **11**, 2727 (1994).
6. J. J. Duderstadt and L. J. Hamilton, *Nuclear Reactor Analysis* (Wiley, New York, 1976).
7. K. Furutsu and Y. Yamada, "Diffusion Approximation for a Dissipative Random Medium and the Applications," *Phys. Rev. E* **50**, 3634-3640 (1994).
8. S. A. Walker, S. Fantini, and E. Gratton, "Analytic Solution for Photon Density Waves Scattering from Cylindrical Inhomogeneities in Turbid Media," in preparation.
9. D. A. Boas, M. A. O'Leary, B. Chance, and A. G. Yodh, "Scattering of Diffuse Photon Density Waves by Spherical Inhomogeneities Within Turbid Media: Analytic Solution and Applications," *Proc. Natl. Acad. Sci. USA* **91**, 4887-4891 (1994).
10. A. H. Hielscher, F. K. Tittel, S. L. Jacques, "Photon Density Wave Diffraction Tomography," *OSA Proceedings on Advances in Optical Imaging and Photon Migration*, R.R. Alfano, ed. (Optical Society of America, Washington D.C. 1994) **21**, 78-82.
11. S. Fantini, M. A. Franceschini, J. B. Fishkin, B. Barbieri, and E. Gratton, "Quantitative Determination of the Absorption Spectra of Chromophores in Strongly Scattering Media: a Light-Emitting-Diode Based Technique," *Appl. Opt.* **33**, 5204-5213 (1994).
12. S. Fantini, M. A. Franceschini, and E. Gratton, "Semi-Infinite-Geometry Boundary Problem for Light Migration in Highly Scattering Media: a Frequency-Domain Study in the Diffusion Approximation," *J. Opt. Soc. Am. B* **11**, 2128-2138 (1994).
13. P. R. Bevington, *Data Reduction and Error Analysis for the Physical Sciences*, (McGraw Hill, New York, 1969).